

PAPER • OPEN ACCESS

## Automatic defect detection from thermographic non destructive testing

To cite this article: G. Dinardo *et al* 2019 *J. Phys.: Conf. Ser.* **1249** 012010

View the [article online](#) for updates and enhancements.



**IOP | ebooks™**

Bringing you innovative digital publishing with leading voices to create your essential collection of books in STEM research.

Start exploring the [collection](#) - download the first chapter of every title for free.

# Automatic defect detection from thermographic non destructive testing

G. Dinardo, L. Fabbiano, R. Tamborrino, G. Vacca

Mechanics, Mathematics and Management Department, Polytechnic of Bari,  
University

giuseppe.dinardo@poliba.it

**Abstract.** This paper illustrates an innovative algorithm for the detection and localization of partial detachment defects affecting thermal barrier coatings (TBCs), using the Long Pulsed Thermography (LPT). The scientific literature offers many applications, proving the LPT effectiveness in providing clear and intelligible thermal image contrasts. The proposed post processing technique directly operates on the raw thermograms acquired from the specimen surface. The algorithm aims at improving the polynomial fit of the logarithmic time history of the surface temperature during the cooling stage. The enhancements consist of the introduction of additional parameters, such as the fit zero-intercept and its standard deviation whose efficiencies are compared with the already exploited fit slope and determination coefficient ones. The considered parameters, called damage classifiers, are set in image maps from which the possible defects are deducted.

## 1. Introduction

In recent years, thermography has appeared particularly attractive among the nondestructive testing (NDT) methods for the detection of defects in materials. It offers the advantages of low cost, easy operation, high speed, and wide area coverage.

The most widely used form of thermographic NDT is the pulsed thermography in which the surface of a tested part is heated by a brief pulse of light usually from a high power source. Along with pulsed thermography, the step heating technique has recently received more attention. It is implemented by applying a thermal stimulation to a surface for more than few milliseconds [1,2]. The time-dependent surface temperature response is captured as a series of thermal images by an infrared camera, [3]. The temperature contrast between the defective and non-defective regions enables the defect detection based on thermographic data. However, thermal images usually involve significant measurement noise and non-uniform backgrounds caused by uneven heating, [4]. Hence, different types of thermographic image analysis methods have been proposed for signal enhancement [5-9].

In this paper, the authors introduce a new processing technique of the thermographic data, obtained using the stepped thermography, for the detection of possible defects. The technique includes a series of enhancements of the linear fit of the log-log cooling time history of the specimen surface temperature. Basically, the algorithm is directly applied to the thermographic images indicating the temperature trend of each pixel. The slope ( $m$ ) of the linear fit of the log-log of the surface temperature time history is going to be used as a primary indicator of the location and size of the defects. The idea inspiring this work is to significantly enhance the fit, adopting optimization techniques to better utilize the spatial



information coming from the thermographic data. Besides, additional rigorous parameters will be proposed to accurately evaluate a defect.

## 2. Experimental setup

The study has been conducted using experimental data from a campaign of measurements carried out on thermal barrier coatings (TBCs). The defect on which it has been focused the attention is the debonding between the coating and the substrate which is one of the common structural defects of TBCs [10]. Three identical primary specimens are characterized by a circular defect (emulating a partial detachment of the thermal coating) of varying diameter: 2mm (specimen A), 3mm (specimen D), and 5mm (specimen E), (figure 1 a-b).



1a



1b

**Figure 1.** 1a. Picture of one of the reference-coated samples; 1b. Picture of a sample during the phase for producing the adhesion defect

A 1064 nm wavelength Ytterbium pulsed fiber laser for implementing the stepped thermography has been used and a cooled IR camera with an Indium-Antimony detector to monitor the thermal transient of the sample surface. The experimental set up is shown in figure 2.

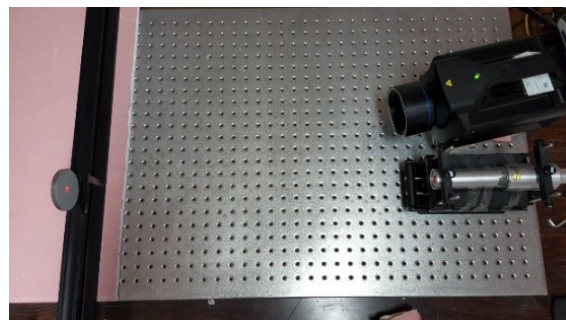
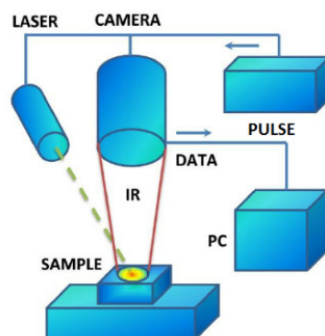


**Figure 2.** Experimental set up for thermographic data acquisition

## 3. Proposed algorithm description and preliminary results

The flowchart of the proposed post-processing algorithm is shown in figure 3. The algorithm consists of a series of enhancements of the linear fit of the cooling curve (in log-log scale) [11].

The significant parameters deriving from the linear least squares fit performed on each pixel are the slope ( $m$ ) and the fit autocorrelation coefficient ( $R^2$ ). These parameters, as pointed out in [10], provide qualitative information about any possible defect location and size. Additionally, the authors of this paper introduce the fit standard deviation ( $S_p$ ) and fit intercept ( $q$ ). The obtained results have been compared with those deriving from the Thermographic Signal Reconstruction algorithm, TSR [5-7]. The outcome of the algorithm consists of a series of images indicating the amount of the fit parameters for each pixel. Figure 4 and 5 show the TSR coefficient maps and the linear fit parameters (as proposed in this paper) for specimen A. The quantities represented in the images related to linear fit parameters are:  $\text{abs}(\text{sound\_zone\_value} - \text{defect\_zone\_value}) / \text{sound\_zone\_value}$  for each parameter. The white color indicates the non-defective pixels, the darker ones (with relative values tending to 0) indicate pixels with defects. Figure 6 and figure 7 are relative to specimen D, while figure 8 and figure 9 refer to specimen E.

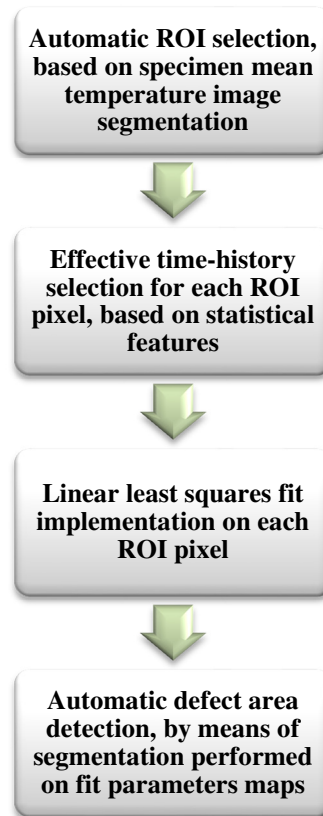


**Figure 3.** Flowchart of the proposed algorithm

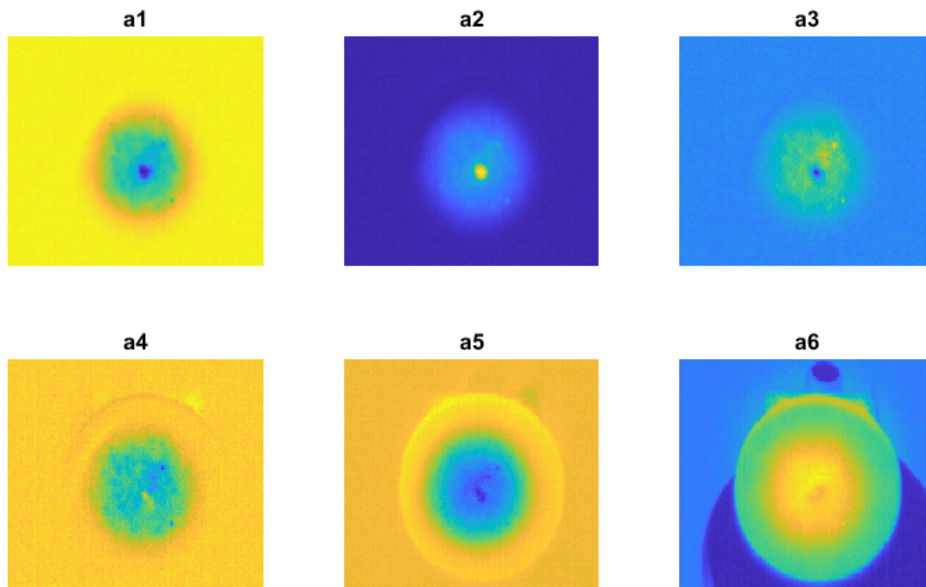


**Figure 4.** Coefficient maps from TRS algorithm, specimen A

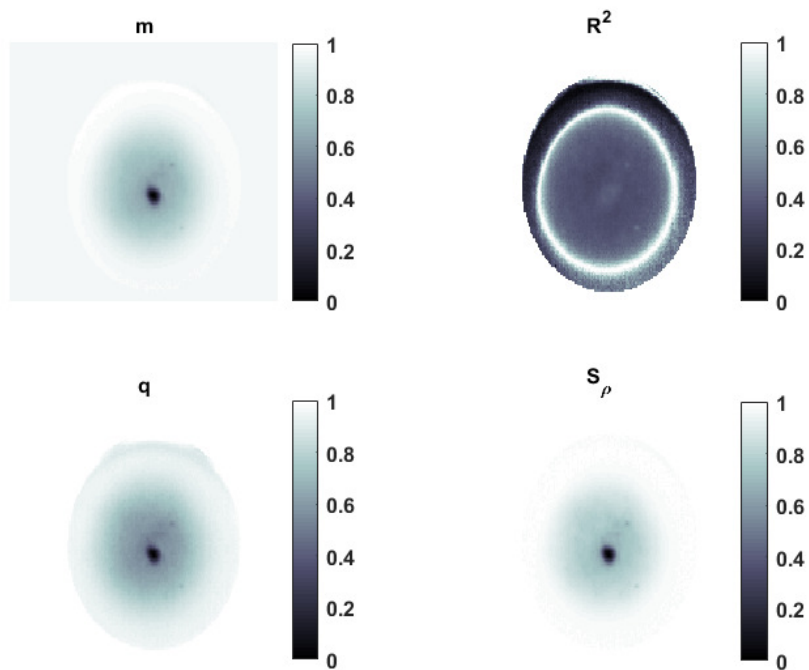


**Figure 5.** Linear fit coefficients, according to the proposed techniques ( $q$  and  $S_\rho$ ) compared with literature algorithms ( $m$  and  $R^2$ ), for specimen A

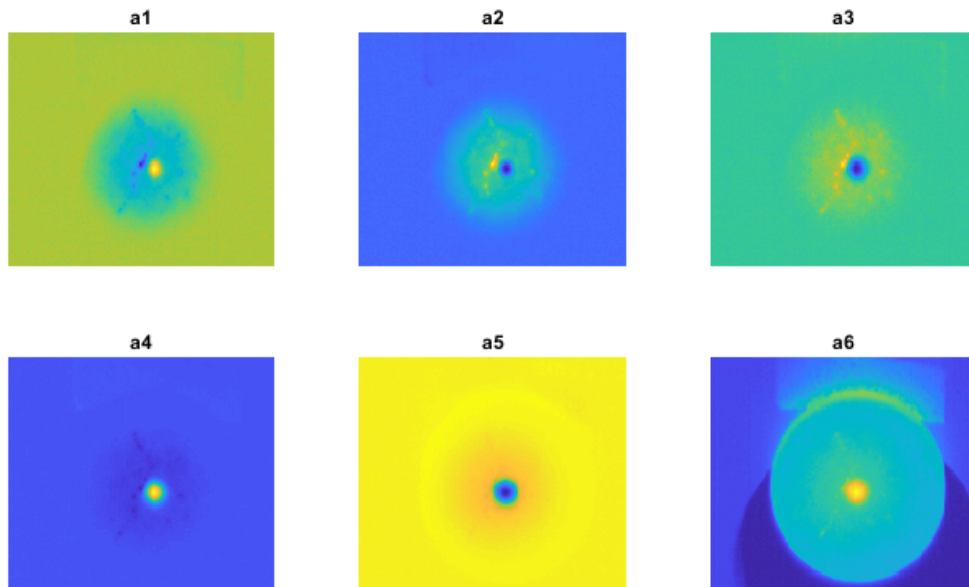


**Figure 6.** Coefficient maps from TRS algorithm, specimen D

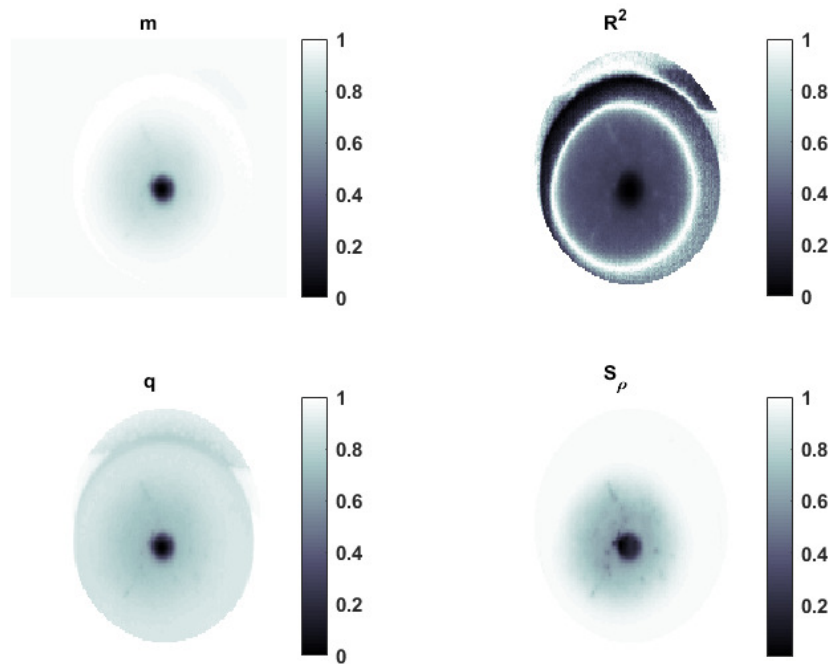


**Figure 7.** Linear fit coefficients, according to the proposed techniques ( $q$  and  $S_p$ ) compared with literature algorithms ( $m$  and  $R^2$ ), for specimen D

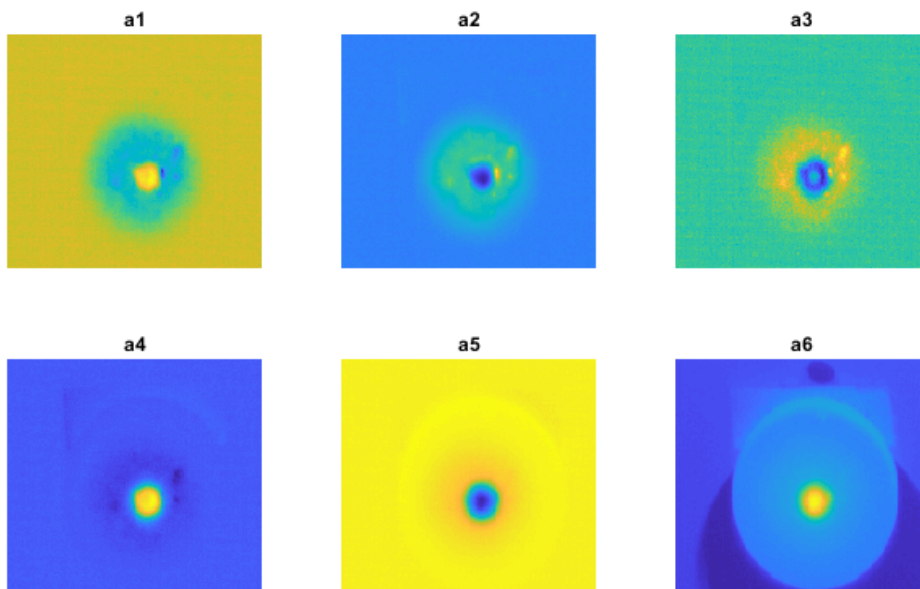


**Figure 8.** Coefficient maps from TRS algorithm, specimen E

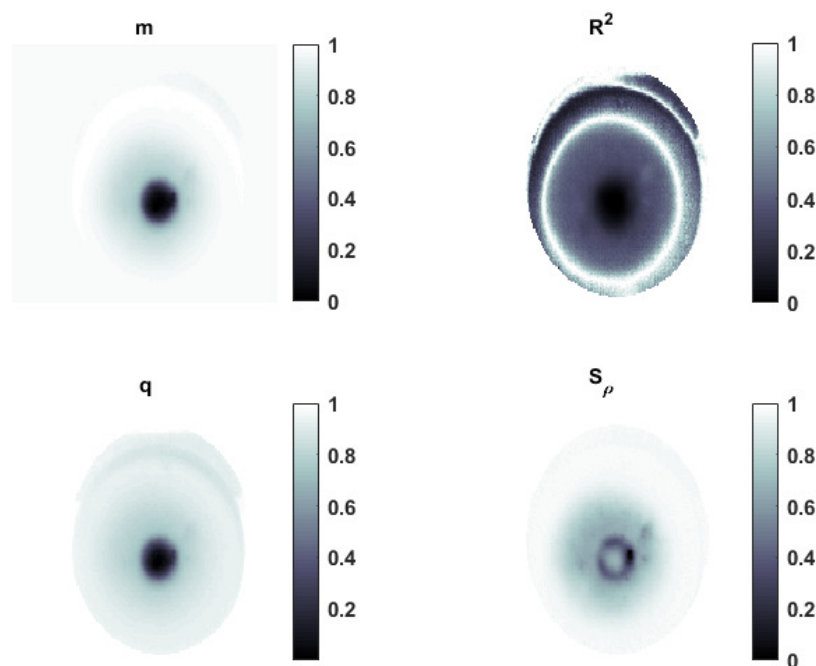


**Figure 9.** Linear fit coefficients, according to the proposed techniques ( $q$  and  $S_p$ ) compared with literature algorithms ( $m$  and  $R^2$ ), for specimen E

Figure 5 and figure 7 show equivalent features of the  $m$ ,  $q$  and  $S_p$  parameters, certainly better than  $R^2$  for sharpness and for sizing the defect, at least from a qualitative point of view.

In figure 9 the comparison still shows such a superiority, except that the  $S_p$  parameter, due to an insufficient time for the diffusion of heat transfer towards the inner zone of the defect (because of different its conductivity properties) with the increase of its size, show a still unheated area there, while correctly estimating its external size.

A further segmentation can be then implemented on the achieved images. This step allows for the detection of the damaged pixels and, therefore, a quantitative defect characterization is possible.

So, a quantitative analysis and evaluations of these qualitative observations will be assessed in a next paper, where an estimation of the uncertainty of the defect size will be provided.

#### 4. Conclusion

In this paper new damage classifiers are proposed able to detecting and sizing subsurface defects of partial detachments of TBCs from the primary metallic substrate. Such classifiers are expressions of an algorithm that directly processes the thermograms representing the time evolution of the sample surface temperature under inspection. The algorithm works without any a priori knowledge about pixel distributions between the back- and fore-ground regions and those ones between defect and sound regions within the identified foreground. Three specimens (round disks of subsurface defects different in size), based on same components, have been inspected and tested by acquiring images with Long Pulse Thermography technique.

Such images have been processed with the proposed algorithm so defining the new indexes,  $q$  and  $S_p$ , compared with those ones,  $m$  and  $R^2$ , already present in literature for such a kind of processing.

The classifiers are then organized in image maps whose pixel' luminance indicates the classifiers distributions to show the presence of the defect in the specimens. From a qualitative point of view,  $q$ ,  $S_p$  and  $m$  have presented equivalent better features respect to the  $R^2$  index in general. A further development of the proposed post processing technique has allowed a quantification of the defect size from the damage classifiers maps (by means of post segmentation implementation) with high accuracy and precision and, in addition, the identification of the best performing classifier. That will be discussed in a next paper about this subject.

#### References

- [1] Balageas D L and Roche J M 2014 Common tools for quantitative time-resolved pulse and step-heating thermography - Part I: Theoretical basis. *Quantitative InfraRed Thermography Journal*, 11(1), 43–56. <http://doi.org/10.1080/17686733.2014.891324>
- [2] Roche J M and Balageas D L 2015 Common tools for quantitative pulse and step-heating thermography - Part II: Experimental investigation. *Quantitative InfraRed Thermography Journal*, 12(1), 1–23. <http://doi.org/10.1080/17686733.2014.996341>
- [3] Vavilov V P and Burleigh D D 2015 Review of pulsed thermal NDT: Physical principles, theory and data processing. *NDT and E International*.
- [4] Zheng K Chang Y S and Yao Y 2015 Defect detection in CFRP structures using pulsed thermographic data enhanced by penalized least squares methods. *Composites Part B: Engineering*, 79, 351–358. <http://doi.org/10.1016/j.compositesb.2015.04.049>
- [5] Shepard S M 2001 Advances in Pulsed Thermography. In *Proceedings of SPIE* (Vol. 4360, pp. 511–515). <http://doi.org/10.1117/12.421032>
- [6] Shepard S M Lhota J R Rubadeux B A Ahmed T and Wang D 2002 Enhancement and reconstruction of thermographic NDT data. In *Proceedings of SPIE* (Vol. 4710, pp. 531–535). <http://doi.org/10.1117/12.459603>
- [7] Maldague X Galmiche F and Ziadi A 2002 Advances in pulsed phase thermography. *Infrared Physics and Technology*, 43(3–5), 175–181. [http://doi.org/10.1016/S1350-4495\(02\)00138-X](http://doi.org/10.1016/S1350-4495(02)00138-X)
- [8] Ibarra-Castaneda C and Maldague X 2004 Pulsed phase thermography reviewed. *Quantitative InfraRed Thermography Journal*, 1(1), 47–70. <http://doi.org/10.3166/qirt.1.47-70>
- [9] Rajic N 2002 Principal component thermography for flaw contrast enhancement and flaw depth characterisation in composite structures. *Composite Structures*, 58(4), 521–528.



[http://doi.org/10.1016/S0263-8223\(02\)00161-7](http://doi.org/10.1016/S0263-8223(02)00161-7)

- [10] Palumbo D Tamborrino R and Galietti U 2017 Coating defect evaluation based on stimulated thermography. In Proceedings of SPIE - The International Society for Optical Engineering (Vol. 10214). <http://doi.org/10.1117/12.2267851>
- [11] Otsu N 1979 A threshold selection method from gray level histograms. IEEE Trans. Systems, Man and Cybernetics, 9, 62–66. <http://doi.org/10.1109/TSMC.1979.4310076>